Steel and Composite Structures, *Vol. 33, No. 2 (2019) 307-318*
DOI: https://doi.org/10.12989/scs.2019.33.2.307

Nonlinear bending analysis of porous FG thick annular/circular nanoplate based on modified couple stress and two-variable shear deformation theory using GDQM

Amirmahmoud Sadoughifar [1], Fatemeh Farhatnia*[1,2], Mohsen Izadinia [1] and Sayed Behzad Talaeitaba [1,3]

[1] *Department of Civil Engineering, Najafabad Branch, Islamic Azad University, Najafabad, Isfahan, Iran, 8514143131, Iran*
[2] *Department of Mechanical Engineering, Khomeinishahr Branch, Islamic Azad University, Khomeinishahr, Isfahan, Iran, 8418148499, Iran*
[3] *Department of Civil Engineering, Khomeinishahr Branch, Islamic Azad University, Khomeinishahr, Isfahan, Iran*

(*Received June 30, 2019, Revised September 25, 2019, Accepted September 27, 2019*)

Abstract. This is the first attempt to consider the nonlinear bending analysis of porous functionally graded (FG) thick annular and circular nanoplates resting on Kerr foundation. The size effects are captured based on modified couple stress theory (MCST). The material properties of the porous FG nanostructure are assumed to vary smoothly through the thickness according to a power law distribution of the volume fraction of the constituent materials. The elastic medium is modeled by Kerr elastic foundation which consists of two spring layers and one shear layer. The governing equations are extracted based on Hamilton's principle and two variables refined plate theory. Utilizing generalized differential quadrature method (GDQM), the nonlinear static behavior of the nanostructure is obtained under different boundary conditions. The effects of various parameters such as material length scale parameter, boundary conditions, and geometrical parameters of the nanoplate, elastic medium constants, porosity and FG index are shown on the nonlinear deflection of the annular and circular nanoplates. The results indicate that with increasing the material length scale parameter, the nonlinear deflection is decreased. In addition, the dimensionless nonlinear deflection of the porous annular nanoplate is diminished with the increase of porosity parameter. It is hoped that the present work may provide a benchmark in the study of nonlinear static behavior of porous nanoplates.

Keywords: nonlinear bending; FG porous; annular and circular nanoplates; modified couple stress theory; Kerr medium

1. Introduction

The functionally graded (FG) nanostructures as an advanced product of composite structures have widespread applications in nano-mechanical systems. One of the important kinds of nanostructures is nanoplates with different applications in solar cells. In the FG nanoplates, the material properties are varied gradually from one surface to another. However, adding the FG layer in the arbitrary direction is gradually reduced the stress discontinuity in the same direction. This kind of the materials are generally nonhomogeneous and isotropic, which are made from a mixture of metals and ceramics to obtain a composition that possesses a desirable application, particularly in thermal environments, which leads to extend the application of these nanostructures.

The dynamic and static responses of nanoplates have been received the great deal of attention of the researchers in scientific investigations. Narendar and Gopalakrishnan (2012) presented the buckling analysis of orthotropic nanoplates such as graphene using the two-variable refined plate theory and nonlocal small-scale effects. Malekzadeh and Shojaee (2013a) employed a two-variable first-order shear deformation theory in combination with surface free energy and small scale effect to present a free vibration of nanoplates with arbitrary boundary conditions. Based on a modified couple stress theory, a model for sigmoid functionally graded material (S-FGM) nanoplates resting on elastic medium was developed by Jung *et al*. (2014). Karlicic *et al*. (2015) introduced to non-local elasticity theory for static, dynamic and stability analysis in a wide range of nanostructures. Bending, buckling and vibration of nanobeams and nanoplates subjected to different sets of boundary conditions based on various nonlocal theories were presented by Chakraverty and Behera (2016). Shokrani *et al*. (2016) presented a numerical solution for buckling analysis of double orthotropic nanoplates (DONP) embedded in elastic media under biaxial, uniaxial and shear loading numerically. Vibration of orthotropic double-layered graphene sheets under hygrothermal conditions was investigated by Sobhy (2016) using the trigonometric shear deformation plate theory and Eringen model. Karami and Janghorban (2016) examined the effect of magnetic field on the wave propagation in rectangular nanoplates based on two-variable refined plate theory. The buckling analysis of FG circular/annular nanoplates under uniform in-plane radial compressive load with a concentric internal ring support and elastically restrained edges was examined by Bedroud *et al*. (2016) using an exact analytical approach

*Corresponding author, Professor,
E-mail: farhatnia@iaukhsh.ac.ir; zh_farhat@yahoo.com

http://www.techno-press.org/?journal=scs&subpage=6
ISSN: 1229-9367 (Print), 1598-6233 (Online)

within the framework of nonlocal Mindlin plate theory. Buckling of functionally graded (FG) single-layered annular graphene sheets embedded in a Pasternak elastic medium was investigated by Golmakani and Vahabi (2017) using the nonlocal elasticity theory. The influence of temperature change on the vibration, buckling, and bending of orthotropic graphene sheets embedded in elastic media including surface energy and small-scale effects was investigated by Karimi and Shahidi (2017). Free vibration behavior of functionally nanoplate resting on a Pasternak linear elastic foundation was investigated by Ebrahimi and Heidari (2017). The wave propagation technique was developed by Bahrami and Teimourian (2017) for analyzing the wave power reflection in circular annular nanoplates. Forced vibration behavior of porous metal foam nanoplates on elastic medium was studied by Barati (2017a) via a 4-variable plate theory. Hygro-thermo-mechanical vibration and buckling of exponentially graded (EG) nanoplates resting on two-parameter Pasternak foundations were studied by Sobhy (2017) using the four-unknown shear deformation plate theory. An exact analytical approach based on Mindlin plate theory was considered by Rezaei and Saidi (2018) for free vibration analysis of fluid-saturated porous annular sector plates. Eringen nonlocal elasticity theory in conjunction with surface elasticity theory was employed by Ebrahimi and Heidari (2018) to study nonlinear free vibration behavior of FG nano-plate lying on elastic foundation, on the base of Reddy\'s plate theory. A high-order nonlocal strain gradient model was developed by Shahsavari *et al*. (2018) for wave propagation analysis of porous FG nanoplates resting on a gradient hybrid foundation in thermal environment. A new size-dependent quasi-3D plate theory was presented by Karami *et al*. (2018) for wave dispersion analysis of functionally graded nanoplates while resting on an elastic foundation and under the hygrothermaal environment.

There are vast researches for the static and dynamic responses of nano and macro structures by numerical and analytical methods. Phadikar and Pradhan (2010) and Xu *et al*. (2016) employed numerical approach for vibration response of nonlocal elastic nanobeams/nanoplates and double-layered graphene sheets, respectively. The Navier method was used by Narendar (2011) for buckling analysis of micro-/nano-scale plates, Malekzadeh and Shojaee (2013b) for free vibration of nanoplates.

The Runge-Kutta and Bubnov-Galerkin methods were used by Duc (2013) for nonlinear dynamic response of imperfect eccentrically stiffened FG double curved shallow shells, Quan *et al*. (2015) for nonlinear dynamic analysis and vibration of shear deformable eccentrically stiffened S-FG cylindrical panels, Duc (2016) for nonlinear thermal dynamic analysis of eccentrically stiffened S-FGM circular cylindrical shells, Duc *et al*. (2018) for nonlinear thermo-mechanical response of eccentrically stiffened Sigmoid FGM circular cylindrical shells, Chan *et al*. (2019) for vibration and nonlinear dynamic response of eccentrically stiffened FG composite truncated conical shells

Abbasi *et al*. (2014) concerned with static analysis of functionally graded (FG) circular plates resting on Winkler elastic foundation. Thermal buckling analysis of a FG circular plate exhibiting polar orthotropic characteristics and resting on the Pasternak elastic foundation was presented by Farhatnia *et al*. (2017) using differential transform method. Element based differential quadrature method (EDQM) was applied by Rajasekaran (2017) to analyze static, stability and free vibration of non-homogeneous orthotropic rectangular plates of variable or stepped thickness. DQM is applied for Nonlinear vibration analysis of a nonlocal sinusoidal shear deformation carbon nanotubes by Rahimi Pour *et al*. (2015), vibration of axially moving viscoelastic plate By Robinson (2018) vibration frequency of orthotropic nanoplate by Ghadiri *et al*. (2017), nonlinear bending of FG circular plates by Farhatnia *et al*. (2018) and buckling of rectangular plates by Poodeh *et al*. (2018), thermo elasticity solution of functionally graded, solid, circular, and annular plates integrated with piezoelectric layers by Alibeigloo (2018).

To the best knowledge of authors, no published work has been devoted to nonlinear bending of FG porous annular/circular nanoplates by considering the influence of three-parameter (Kerr) elastic foundation. To this end, we accomplished the nonlinear bending analysis of FG porous annular/circular nanoplates based on two variables refined plate theory. Shimpi and Patel (2006) was the first scholar who developed the two-variable plate theory for isotropic plates. MCST is used for capturing the size effects and the elastic medium is simulated by Kerr foundation. The major role of the third foundation parameter in Kerr foundation model improves the flexibility in controlling the degree of foundation-surface continuity between the loaded and the unloaded regions of the structure-foundation system (Limkatanyu *et al*. 2013). Herein, the solution procedure GDQM is employed in obtaining the nonlinear displacement and stress distribution of the nanostructure under different edge conditions in inner and outer boundaries of annular and circular plates. The influences of different parameters such as material length scale parameter, boundary conditions, and geometrical parameters of the nanoplate, elastic medium constants, porosity and FG power index are exhibited on the nonlinear static behavior of the annular/circular nanoplates.

2. Formulation

Figs. 1 and 2 show an annular and circular FG porous nanoplate, respectively. The circular nanoplate has radius of R and thickness of h which the annular one has inner radius of R_i, outer radius of R_o and thickness of h. The nanostructure is subjected to a uniform constant transverse loading and resting on Kerr foundation with upper and lower springs as well as a shear layer.

2.1 Two refined plate theory

Based on two refined plate theory, the displacements of the structure with assumption of symmetric condition in the nanoplate can be written as (Shimpi and Patel 2006)

$$U(r,z) = u(r) - z\frac{dw_b(r)}{dr} + f(z)\frac{dw_s(r)}{dr}, \tag{1}$$

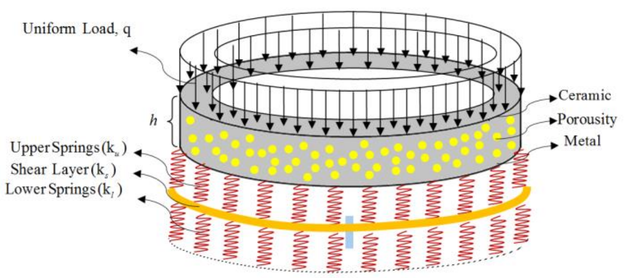

Fig. 1 A schematic of annular FG porous nanoplate resting on Kerr foundation

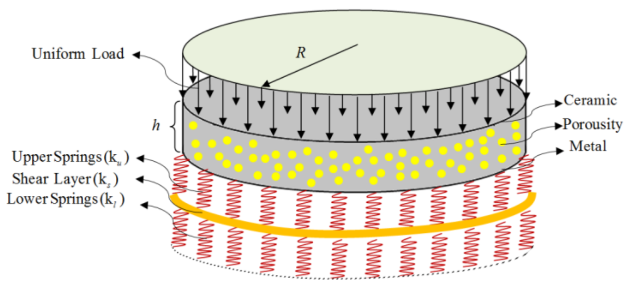

Fig. 2 A schematic of circular FG porous nanoplate resting on Kerr foundation

$$V(r,z) = 0, \tag{2}$$

$$W(r,z) = w_b(r) + w_s(r), \tag{3}$$

where U, V and W are displacements in the axial, circumferential and transverse directions, respectively; u, w_b and w_s are mid-plane axial, transverse bending and transverse shear displacements, respectively and $f(z) = z\left[1 + \frac{3\pi}{2} sec\,h^2\left(\frac{1}{2}\right)\right] - \frac{3\pi}{2} h\,tanh\left(\frac{z}{h}\right)$.

2.2 Modified Couple Stress Theory (MCST)

According with this theory, the strain energy is written as a function of strain tensor ($\boldsymbol{\varepsilon_{ij}}$) and symmetric curvature tensor ($\boldsymbol{\chi_{ij}}$) (Jung *et al*. 2014)

$$U_b = \frac{1}{2}\int_V (\sigma_{ij}\varepsilon_{jk} + m_{ij}\chi_{ij})dV, \tag{4}$$

where

$$\varepsilon_{ij} = \frac{1}{2}\left(\frac{\partial u_j}{\partial x_i} + \frac{\partial u_i}{\partial x_j}\right), \tag{5}$$

$$\chi_{ij} = \frac{1}{2}\left(\frac{\partial \theta_i}{\partial x_j} + \frac{\partial \theta_j}{\partial x_i}\right), \tag{6}$$

where $u = [U, V, W]$ and θ is the rotation vector which can be defined as

$$\theta_i = \frac{1}{2} e_{ijk}\frac{\partial u_k}{\partial x_j} = \frac{1}{2}\nabla\times \mathrm{u}, \tag{7}$$

where $e_{ijk}$is the components of permutation tensor. The Cartesian components of the stress tensor ($\boldsymbol{\sigma_{ij}}$) and the deviatoric part of the symmetric couple stress tensor ($\boldsymbol{m_{ij}}$) are

$$\sigma_{ij} = K\delta_{ij}\varepsilon_{mm} + 2G\varepsilon_{ij}, \tag{8}$$

$$m_{ij} = 2l_0^2 G\chi_{ij}, \tag{9}$$

in which l_0 is the material length scale parameter; K and G are bulk and shear modulus, respectively which can be expressed in term of Young' modulus (E) and Poisson's ratio ($\boldsymbol{\nu}$) as

$$K = \frac{E\nu}{(1+\nu)(1-2\nu)}, \tag{10}$$

$$G = \frac{E}{2(1+\nu)}. \tag{11}$$

Substituting Eqs. (1)-(3) into Eqs. (5) and (6), the non-zero components of strain and curvature tensors are

$$\varepsilon_{rr} = \frac{du}{dr} - z\frac{d^2w_b}{dr^2} + f(z)\frac{d^2w_s}{dr^2} + \frac{1}{2}\left(\frac{dw_b}{dr} + \frac{dw_s}{dr}\right)^2, \tag{12}$$

$$\varepsilon_{\theta\theta} = \frac{u}{r} - \frac{z}{r}\frac{dw_b}{dr} + \frac{f(z)}{r}\frac{dw_s}{dr}, \tag{13}$$

$$\varepsilon_{rz} = \frac{dw_s}{dr} + \frac{df(z)}{dz}\frac{dw_s}{dr}. \tag{14}$$

$$\begin{aligned}\chi_{r\theta} = &-\frac{d^2w_b}{dr^2} + \frac{1}{2}\frac{df(z)}{dz}\frac{d^2w_s}{dr^2} - \frac{1}{2}\frac{d^2w_s}{dr^2}\\ &+\frac{1}{r}\frac{dw_b}{dr} + \frac{1}{2r}\frac{dw_s}{dr} - \frac{1}{2r}\frac{df(z)}{dz}\frac{dw_s}{dr},\end{aligned} \tag{15}$$

$$\chi_{z\theta} = \frac{1}{2}\frac{d^2f(z)}{dz^2}\frac{dw_s}{dr}. \tag{16}$$

Substituting Eqs. (1)-(3) into Eqs. (8) and (9), the non-zero components of Cartesian stress and deviatoric part of the symmetric couple stress tensors are

$$\sigma_{rr} = \frac{E}{1-\nu^2}\left(\begin{array}{l}\left(\begin{array}{l}\frac{du}{dr} - z\frac{d^2w_b}{dr^2} + f(z)\frac{d^2w_s}{dr^2}\\ +\frac{1}{2}\left(\frac{dw_b}{dr} + \frac{dw_s}{dr}\right)^2\end{array}\right)\\ +\nu\left(\frac{u}{r} - \frac{z}{r}\frac{dw_b}{dr} + \frac{f(z)}{r}\frac{dw_s}{dr}\right)\end{array}\right), \tag{17}$$

$$\sigma_{\theta\theta} = \frac{E}{1-\nu^2}\left(\begin{array}{l}\nu\left(\begin{array}{l}\frac{du}{dr} - z\frac{d^2w_b}{dr^2} + f(z)\frac{d^2w_s}{dr^2}\\ +\frac{1}{2}\left(\frac{dw_b}{dr} + \frac{dw_s}{dr}\right)^2\end{array}\right)\\ +\left(\frac{u}{r} - \frac{z}{r}\frac{dw_b}{dr} + \frac{f(z)}{r}\frac{dw_s}{dr}\right)\end{array}\right), \tag{18}$$

$$\sigma_{rz} = \frac{E}{2(1+\nu)}\left(\frac{dw_s}{dr} + \frac{df(z)}{dz}\frac{dw_s}{dr}\right). \tag{19}$$

$$m_{r\theta}=2l_0G\left(-\frac{d^2w_b}{dr^2}+\frac{1}{2}\frac{df(z)}{dz}\frac{d^2w_s}{dr^2}-\frac{1}{2}\frac{d^2w_s}{dr^2}\right.\\ \left.+\frac{1}{r}\frac{dw_b}{dr}+\frac{1}{2r}\frac{dw_s}{dr}-\frac{1}{2r}\frac{df(z)}{dz}\frac{dw_s}{dr}\right), \tag{20}$$

$$m_{z\theta}=2l_0G\left(\frac{1}{2}\frac{d^2f(z)}{dz^2}\frac{dw_s}{dr}\right). \tag{21}$$

2.3 The effective material property of FG porous nanoplate

Based on the modified power-law model, Young's modulus can be described as (Barati 2017b)

$$E(z)=(E_c-E_m)\left(\frac{z}{h}+\frac{1}{2}\right)^p+E_m-\frac{\xi}{2}(E_c+E_m), \tag{22}$$

where the m and c indexes are related to metal and ceramic, respectively; p is the nonhomogeneous parameter and $\boldsymbol{\xi}$ shows the porosity of the structure.

2.4 Governing equations

To establish the governing equilibrium equations for the annular/circular FG porous thick nanoplate resting on the Kerr foundation, herein we use the Hamilton's principle as

$$\boldsymbol{\int_0^t(\delta\Pi)dt=\int_0^t-(\delta U_b+\delta W_e+\delta W_b)dt=0.} \tag{23}$$

where δ is variation operator; Π denotes the total potential energy of the nanostructure; U_b, W_e and W_b represent the bending strain energy, the Kerr foundation energy, and the potential of external work done by uniform constant transverse load, respectively. By utilizing δ in the above-mentioned parameters, we have

$$\delta U_b=\int_V\begin{pmatrix}\sigma_{rr}\delta\varepsilon_{rr}+\sigma_{\theta\theta}\delta\varepsilon_{\theta\theta}+\sigma_{rz}\delta\varepsilon_{rz}\\ +m_{r\theta}\delta\chi_{r\theta}+m_{z\theta}\delta\chi_{z\theta}\end{pmatrix}rdrd\theta dz' \tag{24}$$

$$\delta W_e=\int_A q_{Kerr}\,\delta\,Wrdrd\theta. \tag{25}$$

$$\delta W_b=-\int_A q\,\delta\,Wrdrd\theta. \tag{26}$$

where q is the transverse load applied to the annular/circular nanoplate and q_{Kerr} is the force of the Kerr foundation which can be expressed as (Paliwal and Ghosh 2014)

$$q_{Kerr}-\left(\frac{k_s}{k_l+k_u}\right)\nabla^2 q_{Kerr}=\left(\frac{k_lk_u}{k_l+k_u}\right)\\ (w_b+w_s)-\left(\frac{k_sk_u}{k_l+k_u}\right)\nabla^2(w_b+w_s). \tag{27}$$

Substituting Eqs. (12)-(16) into Eq. (24) and carrying out some mathematical simplification, yields

$$\delta U_b=2\pi\int_V\left[rN_r\begin{pmatrix}\frac{d\delta u}{dr}+\frac{dw_b}{dr}\frac{d\delta w_b}{dr}+\frac{dw_s}{dr}\frac{d\delta w_s}{dr}\\ +\frac{dw_s}{dr}\frac{d\delta w_b}{dr}+\frac{d\delta w_s}{dr}\frac{dw_b}{dr}\end{pmatrix}\right.\\ +N_\theta(\delta u)+rN_{rz}\left(\frac{d\delta w_s}{dr}\right)+rQ_{rz}\left(\frac{d\delta w_s}{dr}\right)\\ -rM_{rb}\left(\frac{d^2\delta w_b}{dr^2}\right)+rM_{rs}\left(\frac{d^2\delta w_s}{dr^2}\right)\\ -M_{\theta b}\left(\frac{d\delta w_b}{dr}\right)+M_{\theta s}\left(\frac{d\delta w_s}{dr}\right)\\ +rP_{r\theta}\left(-\frac{d^2\delta w_b}{dr^2}-\frac{1}{2}\frac{d^2\delta w_s}{dr^2}+\frac{1}{r}\frac{d\delta w_b}{dr}+\frac{1}{2r}\frac{d\delta w_s}{dr}\right)\\ \left.+rY_{r\theta}\left(\frac{1}{2}\frac{d^2\delta w_s}{dr^2}-\frac{1}{2r}\frac{d\delta w_s}{dr}\right)+rT_{z\theta}\left(\frac{1}{2}\frac{d\delta w_s}{dr}\right)\right]dr, \tag{28}$$

where the stress resultants are

$$(N_r,M_{rb},M_{rs})=\int_{-h/2}^{h/2}\sigma_{rr}(1,z,f(z))dz, \tag{29}$$

$$(N_\theta,M_{\theta b},M_{\theta S})=\int_{-h/2}^{h/2}\sigma_{\theta\theta}(1,z,f(z))dz, \tag{30}$$

$$(N_{rz},Q_{rz})=\int_{-h/2}^{h/2}\sigma_{rz}\left(1,\frac{df(z)}{dz}\right)dz, \tag{31}$$

$$(P_{r\theta},Y_{r\theta})=\int_{-h/2}^{h/2}m_{r\theta}\left(1,\frac{df(z)}{dz}\right)dz, \tag{32}$$

$$T_{z\theta}=\int_{-h/2}^{h/2}m_{z\theta}\frac{d^2f(z)}{dz^2}dz, \tag{33}$$

Substituting Eqs. (25), (26) and (28) into Eq. (23) integrating the parts, and collecting the coefficients of δu, δw_b, δw_s, the governing equilibrium equations can be obtained as follows

$$\delta u:\quad \frac{1}{r}\left(\frac{d}{dr}(rN_r)-N_\theta\right)=0, \tag{34}$$

$$\delta w_b:\quad \frac{1}{r}\frac{d^2}{dr^2}(rM_{rb})-\frac{1}{r}\frac{dM_{\theta b}}{dr}+\frac{1}{r}\frac{dP_{r\theta}}{dr}\\ +q-q_{Kerr}=0 \tag{35}$$

$$\delta w_s:\quad \frac{1}{r}\frac{dM_{\theta s}}{dr}-\frac{1}{r}\frac{d^2}{dr^2}(rM_{rs})+\frac{1}{r}\frac{d}{dr}(rN_{rz})\\ +\frac{1}{2r}\left(\frac{dP_{r\theta}}{dr}-\frac{dY_{r\theta}}{dr}+\frac{d}{dr}(rT_{z\theta})\right)\\ +\frac{1}{r}\frac{d}{dr}(rQ_{rz})+q-q_{Kerr}=0 \tag{36}$$

substituting q_{Kerr} from Eq. (27) into Eqs. (35) and (36) yields

$$\frac{1}{r}\left(\frac{d}{dr}(rN_r)-N_\theta\right)=0, \tag{37}$$

$$\begin{aligned}&\left(\frac{1}{r}\frac{d^2}{dr^2}(rM_{rb})-\frac{1}{r}\frac{dM_{\theta b}}{dr}+\frac{1}{r}\frac{dP_{r\theta}}{dr}+q\right)\\&-\left(\frac{k_s}{k_l+k_u}\right)\nabla^2\begin{pmatrix}\frac{1}{r}\frac{d^2}{dr^2}(rM_{rb})-\frac{1}{r}\frac{dM_{\theta b}}{dr}\\+\frac{1}{r}\frac{dP_{r\theta}}{dr}+q\end{pmatrix}\\&=\left(\frac{k_lk_u}{k_l+k_u}\right)(w_b+w_s)-\left(\frac{k_sk_u}{k_l+k_u}\right)\nabla^2(w_b+w_s),\end{aligned}\tag{38}$$

$$\begin{aligned}&q_{Kerr}-\left(\frac{k_s}{k_l+k_u}\right)\nabla^2q_{Kerr}=\left(\frac{k_lk_u}{k_l+k_u}\right)\\&(w_b+w_s)-\left(\frac{k_sk_u}{k_l+k_u}\right)\nabla^2(w_b+w_s)\\&+\frac{1}{r}\frac{dM_{\theta s}}{dr}-\frac{1}{r}\frac{d^2}{dr^2}(rM_{rs})+\frac{1}{r}\frac{d}{dr}(rN_{rz})\\&+\frac{1}{2r}\left(\frac{dP_{r\theta}}{dr}-\frac{dY_{r\theta}}{dr}+\frac{d}{dr}(rT_{z\theta})\right)\\&+\frac{1}{r}\frac{d}{dr}(rQ_{rz})+q-q_{Kerr}=0\end{aligned}\tag{39}$$

Substituting Eqs. (12)-(21) into Eqs. (29)-(33), the stress resultants can be expanded as

$$\begin{aligned}N_r=&A\left(\frac{du}{dr}+\frac{1}{2}\left(\frac{dw_b}{dr}+\frac{dw_s}{dr}\right)^2\right)-B\frac{d^2w_b}{dr^2}\\&+F\frac{d^2w_s}{dr^2}+\nu\left(A\frac{u}{r}-\frac{B}{r}\frac{dw_b}{dr}+\frac{F}{r}\frac{dw_s}{dr}\right),\end{aligned}\tag{40}$$

$$\begin{aligned}M_{rb}=&B\left(\frac{du}{dr}+\frac{1}{2}\left(\frac{dw_b}{dr}+\frac{dw_s}{dr}\right)^2\right)-D\frac{d^2w_b}{dr^2}\\&+H\frac{d^2w_s}{dr^2}+\nu\left(B\frac{u}{r}-\frac{D}{r}\frac{dw_b}{dr}+\frac{H}{r}\frac{dw_s}{dr}\right),\end{aligned}\tag{41}$$

$$\begin{aligned}M_{rs}=&F\left(\frac{du}{dr}+\frac{1}{2}\left(\frac{dw_b}{dr}+\frac{dw_s}{dr}\right)^2\right)-H\frac{d^2w_b}{dr^2}\\&+I\frac{d^2w_s}{dr^2}+\nu\left(F\frac{u}{r}-\frac{H}{r}\frac{dw_b}{dr}+\frac{I}{r}\frac{dw_s}{dr}\right),\end{aligned}\tag{42}$$

$$\begin{aligned}N_\theta=&\nu\begin{pmatrix}A\frac{du}{dr}-B\frac{d^2w_b}{dr^2}+F\frac{d^2w_s}{dr^2}\\+\frac{A}{2}\left(\frac{dw_b}{dr}+\frac{dw_s}{dr}\right)^2\end{pmatrix}\\&+A\frac{u}{r}-\frac{B}{r}\frac{dw_b}{dr}+\frac{F}{r}\frac{dw_s}{dr}\end{aligned}\tag{43}$$

$$\begin{aligned}M_{\theta b}=&\nu\begin{pmatrix}B\frac{du}{dr}-D\frac{d^2w_b}{dr^2}+H\frac{d^2w_s}{dr^2}\\+\frac{B}{2}\left(\frac{dw_b}{dr}+\frac{dw_s}{dr}\right)^2\end{pmatrix}\\&+B\frac{u}{r}-\frac{D}{r}\frac{dw_b}{dr}+\frac{H}{r}\frac{dw_s}{dr}\end{aligned}\tag{44}$$

$$\begin{aligned}M_{\theta s}=&\nu\begin{pmatrix}F\frac{du}{dr}-H\frac{d^2w_b}{dr^2}+I\frac{d^2w_s}{dr^2}\\+\frac{F}{2}\left(\frac{dw_b}{dr}+\frac{dw_s}{dr}\right)^2\end{pmatrix}\\&+F\frac{u}{r}-\frac{H}{r}\frac{dw_b}{dr}+\frac{I}{r}\frac{dw_s}{dr}\end{aligned}\tag{45}$$

$$N_{rz}=\frac{(1-\nu)}{2}\left(A\frac{dw_s}{dr}+J\frac{dw_s}{dr}\right).\tag{46}$$

$$Q_{rz}=\frac{(1-\nu)}{2}\left(H\frac{dw_s}{dr}+L\frac{dw_s}{dr}\right).\tag{47}$$

$$\begin{aligned}P_{r\theta}=&l_0(1-\nu)\left(-A\frac{d^2w_b}{dr^2}+\frac{J}{2}\frac{d^2w_s}{dr^2}-\frac{A}{2}\frac{d^2w_s}{dr^2}\right.\\&\left.+\frac{A}{r}\frac{dw_b}{dr}+\frac{A}{2r}\frac{dw_s}{dr}-\frac{J}{2r}\frac{dw_s}{dr}\right),\end{aligned}\tag{48}$$

$$\begin{aligned}Y_{r\theta}=&l_0(1-\nu)\left(-J\frac{d^2w_b}{dr^2}+\frac{L}{2}\frac{d^2w_s}{dr^2}-\frac{M}{2}\frac{d^2w_s}{dr^2}\right.\\&\left.+\frac{M}{r}\frac{dw_b}{dr}+\frac{M}{2r}\frac{dw_s}{dr}-\frac{L}{2r}\frac{dw_s}{dr}\right),\end{aligned}\tag{49}$$

$$T_{z\theta}=l_0(1-\nu)\frac{M}{2}\frac{dw_s}{dr},\tag{50}$$

where

$$\begin{pmatrix}A,B,D,F,H,\\I,J,L,M\end{pmatrix}=\frac{E}{1-\nu^2}\int_{-h/2}^{h/2}\begin{pmatrix}1,z,z^2,f(z),zf(z),\\f(z)^2,\frac{df(z)}{dz}\\,\left(\frac{df(z)}{dz}\right)^2,\frac{d^2f(z)}{dz^2}\end{pmatrix}dz.\tag{51}$$

2.5 Boundary conditions

The boundary conditions for the annular nanoplates at the inner and outer surfaces are

- **Clamped-Clamped (CC)**

$$u=w_b=w_s=\frac{dw_b}{dr}=\frac{dw_s}{dr}=0\quad\text{at}\quad r=R_i,R_o\tag{52}$$

- **Simply-Simply supported (SS)**

$$u=w_b=w_s=M_{rb}=M_{rs}=0\quad\text{at}\quad r=R_i,R_o\tag{53}$$

- **Clamped-Simply supported (CS)**

$$\begin{aligned}&u=w_b=w_s=\frac{dw_b}{dr}=\frac{dw_s}{dr}=0\quad\text{at}\quad r=R_i\\&u=w_b=w_s=M_{rb}=M_{rs}=0\quad at\quad r=R_o\end{aligned}\tag{54}$$

- **Simply- Clamped (SC)**

$$\begin{aligned}&u=w_b=w_s=M_{rb}=M_{rs}=0\quad at\quad r=R_i\\&u=w_b=w_s=\frac{dw_b}{dr}=\frac{dw_s}{dr}=0\quad at\quad r=R_o\end{aligned}\tag{55}$$

- **Clamped-Free (CF)**

$$\begin{aligned}&u=w_b=w_s=\frac{dw_b}{dr}=\frac{dw_s}{dr}=0\quad at\quad r=R_i\\&N_r=N_{rz}=Q_{rz}=M_{rs}=M_{rb}=0\quad at\quad r=R_o\end{aligned}\tag{56}$$

❖ **Free- Clamped (FC)**

$$N_r = N_{rz} = Q_{rz} = M_{rs} = M_{rb} = 0 \quad at \quad r = R_i$$
$$u = w_b = w_s = \frac{dw_b}{dr} = \frac{dw_s}{dr} = 0 \quad at \quad r = R_o \tag{57}$$

Noted that the first boundary condition is related to inner surface of the annular nanoplate and the second ones show the boundary condition of outer surface. For instance, CS boundary conditions indicate clamped edge in the inner surface and simply supported at the outer surface of the annular nanoplate.

The assumed boundary conditions for the circular nanoplates are

❖ **Clamped edge**

$$u = w_b = w_s = \frac{dw_b}{dr} = \frac{dw_s}{dr} = 0 \quad at \quad r = R \tag{58}$$

❖ **Simply supported**

$$u = w_b = w_s = M_{rb} = M_{rs} = 0 \quad at \quad r = R \tag{59}$$

In the center of the circular nanoplate, the below conditions should be satisfied

$$u = \frac{dw_b}{dr} = \frac{dw_s}{dr} = N_{rz} = Q_{rz} = 0 \quad at \quad r = 0 \tag{60}$$

3. Solution method

Based on GDQM, the first and the higher order of derivatives of *f(r)* are approximated by a linear sum of all the function values in the whole domain as follows (Bellman and Casti 1971, Asemi *et al*. 2014, Hajmohammad *et al*. 2018, Dastjerdi *et al*. 2016)

$$\begin{aligned} f^1(r_i) &= \sum_{j=1}^{N_r} C_{ij}^{(1)} f(r_j) \quad \text{for } i = 0, \dots, N_r \\ f_r^{(m-1)}(r_i) &= \sum_{j=1}^{N_r} C_{ij}^{(m-1)} f(r_j) \quad \text{for } i = 1,2,\dots,N_r m \\ &= 2,3,\dots,N_r - 1 \\ f_r^{(m)}(r_i) &= \sum_{j=1}^{N_r} C_{ij}^{(m)} f(r_j) \quad \text{for } i = 1,2,\dots,N_r m \\ &= 2,3,\dots,N_r - 1 \end{aligned} \tag{61}$$

where N_r and r_i are the number of grids and sample points, respectively; $C_{ij}^{(1)}$ and $C_{ij}^{(m)}$ are weighting coefficients, obtained as follows

$$\begin{aligned} C_{ij}^{(1)} &= \frac{M^{(1)}(r_i)}{(r_i - r_j) M^{(1)}(r_j)} \quad \text{for } i \neq j, i,j = 1,2,\dots,N_r \\ C_{ii}^{(1)} &= \frac{M^{(2)}(r_i)}{2M^{(1)}(r_i)} \quad \text{for } i = 1,2,\dots,N_r \\ C_{ij}^{(m-1)} &= \frac{N^{(m-1)}(r_i, r_j)}{M^{(1)}(r_j)} \\ C_{ij}^{(m)} &= \frac{N^{(m)}(r_i, r_j)}{M^{(1)}(r_j)} \end{aligned} \tag{62}$$

where M and N are determined by recurrence relations as follows

$$\begin{aligned} M^{(1)}(r_i) &= \prod_{\substack{k=1 \\ k\neq i}}^{N_r} (r_i, r_k) \\ N^{(m-1)}(r_i, r_j) &= M^{(1)}(r_i) C_{ij}^{(m-1)} \\ N^{(m-1)}(r_i, r_i) &= \frac{M^{(m)}(r_i)}{m} \\ N^{(m)}(r_i, r_j) &= \frac{M^{(m)}(r_i) - m\, N^{(m-1)}(r_i, r_j)}{(r_i - r_j)} \quad \text{for } i \neq j \end{aligned} \tag{63}$$

For optimal selection of the sample points, the normalized Chebyshev–Lobatto points are exploited as respectively for annular and circular nanoplates as (Dastjerdi *et al*. 2016)

$$r_i = \frac{R_o}{2}\left[1 - cos\left(\frac{i-1}{N_r - 1}\right)\pi\right] + R_i i = 1,\dots,N_r \tag{64}$$

$$r = \frac{R}{2}\left[1 - cos\left(\frac{i-1}{N_r - 1}\right)\pi\right] i = 1,\dots,N_r \tag{65}$$

Applying Eq. (61) into Eqs. (37)-(39) yields the final governing equation in matrix form as

$$\begin{bmatrix} K_{bb} & K_{bd} \\ K_{db} & K_{dd} \end{bmatrix} \begin{bmatrix} \{y_b\} \\ \{y_d\} \end{bmatrix} = \begin{bmatrix} \{0\} \\ \{q\} \end{bmatrix}, \tag{66}$$

where $y = [u, w_b, w_s]$; K_{bb} and K_{bd} are stiffness matrixes of boundary and domain points in the boundary equations, respectively; K_{db} and K_{dd} are stiffness matrixes of boundary and domain points in the governing equations, respectively. Finally, using an iterative method, the solution of Eq. (66) yields to the nonlinear displacements of the FG porous annular/circular nanoplate.

4. Numerical results

In this section, the effects of different parameters are shown on the nonlinear displacements of the FG porous nanoplate. For this purpose, the FG nanoplate is consisted of metal and ceramic with Young's modulus of $E_m = 70$ Gpa and $E_c = 151$ Gpa, respectively (Karami and Janghorban 2016). The inner to outer radius of nanoplate is $R_i/R_o = 0.5$ and thickness to outer radius of $h/R_o = 0.1$. For the annular nanoplates, the boundary conditions of CC, SS, CS, SC, CF and FC are considered which the first boundary condition is related to inner surface of the annular nanoplate and the second ones show the boundary condition of outer surface. In addition, for the circular nanoplate two boundary conditions of clamped and simply supported are assumed.

4.1 Validation

Firstly, the results are validated considering the material properties the same as (Saidi *et al*. 2009) neglecting porosity, Kerr foundation and material length scale

Table 1 Non-dimensional deflection of circular FG plate ($W = 64Dw/qR^4$)

BC	p	Ref	*h/R*			
			0.10	0.20	0.35	0.30
Simply supported	0	FSDT (Saidi *et al*. 2009)	4.1502	4.0075	3.9071	3.7905
		TSDT (Ma and Wang 2004)	4.1502	4.0077	3.9072	3.7911
		TSDT (Saidi *et al*. 2009)	4.1503	4.0079	3.9072	3.7911
		Present work	4.1503	4.0078	3.9073	3.7911
	10	FSDT (Saidi *et al*. 2009)	7.9717	7.7149	7.5325	6.3217
		TSDT (Ma and Wang 2004)	7.9733	7.7213	7.5424	6.3353
		TSDT (Saidi *et al*. 2009)	7.9730	7.7211	7.5425	6.3348
		Present work	7.9736	7.7212	7.5427	6.3350
Clamped edge	0	FSDT (Saidi *et al*. 2009)	14.089	12.571	11.631	10.657
		TSDT (Ma and Wang 2004)	14.089	12.574	11.638	10.670
		TSDT (Saidi *et al*. 2009)	14.089	12.575	11.639	10.670
		Present work	14.089	12.575	11.639	10.670
	10	FSDT (Saidi *et al*. 2009)	27.111	24.353	22.627	20.823
		TSDT (Ma and Wang 2004)	27.133	24.423	22.725	20.948
		TSDT (Saidi *et al*. 2009)	27.131	24.422	22.725	20.949
		Present work	27.134	24.423	22.726	20.949

Table 2 Comparison of the maximum dimensionless deflection ($W = 64Dw/qR^4$) of circular FG plate for thickness-to-radius ratio *h/R* = 0.15

FG index	Clamped edge			Simply supported		
	Reddy *et al*. (1999)	Golmakani and Kadkhodayan (2011)	Present	Reddy *et al*. (1999)	Golmakani and Kadkhodayan (2011)	Present
0	2.781	2.774	2.778	10.623	10.572	10.611
2	1.151	1.511	1.512	5.610	5.565	5.577
4	1.384	1.382	1.381	5.271	5.200	5.231
8	1.278	1.277	1.277	4.870	4.876	4.874
10	1.250	1.251	1.252	4.772	4.760	4.770
50	1.137	1.134	1.135	4.348	4.346	4.347
100	1.119	1.116	1.117	4.280	4.281	4.282
1000	1.103	1.107	1.102	4.214	4.229	4.222
10000	1.101	1.102	1.103	4.207	4.217	4.211

parameter, the dimensionless deflection ($W = 64Dw/qR^4$) for the circular plate with simply boundary condition is determined. The results are shown in Table 1 for first order shear deformation theory (FSDT) (Saidi *et al*. 2009), third order shear deformation theory (TSDT) (Ma and Wang 2004) and two refined variable shear deformation theory. As seen, the results are in good agreement with those reported by Saidi *et al*. (2009) and Ma and Wang (2004).

For another validation of this work, the porosity value, Kerr foundation and material length scale parameter are neglected and axisymmetric bending of a FG circular plate with clamped and simply supported boundary conditions is studied based on FSDT. A FGM plate made of a combination of Titanium and Zirconium is considered with $E_c = 151$ Gpa and $E_m/E_c = 0.396$. The dimensionless deflection of the structure for thickness-to-radius ratio of *h/R* = 0.15 is shown in Table 2 and the present results are compared with those obtained by Reddy *et al*. (1999) and Golmakani and Kadkhodayan (2011). Table 2 shows an acceptable agreement on the dimensionless maximum deflection and thus validated of the present numerical method.

For the third validation of this work, the bending of an annular FG plate is investigated for thickness-to-outer radius ratio of *h/R* = 0.15. Herein, the The material properties are assumed to be $E_m = 70$ Gpa, $E_c = 427$ Gpa, $\nu_m = 0.3$ and $\nu_c = 0.17$ for the metal, aluminum, and the ceramic, silicon carbide, respectively. The maximum dimensionless deflection is listed in Table 3 is compared with those reported by Golmakani and Kadkhodayan (2011) for the FSDT and third order shear deformation theory (TSDT). As observed, the present

Table 3 Comparisons of the maximum dimensionless deflection ($W = 64Dw/qR^4$) of SS annular FGM plate

FG power	FSDT (Golmakani and Kadkhodayan 2011)	TSDT (Golmakani and Kadkhodayan 2011)	Present
0	2.45e-3	2.49e-3	2.48e-3
0.1	2.95e-3	2.99e-3	2.98e-3
0.5	3.66e-3	3.70e-3	3.72e-3
1	4.32e-3	4.39e-3	4.31e-3
2	5.16e-3	5.34e-3	5.22e-3
5	6.50e-3	6.88e-3	6.66e-3
Metal	1.58e-2	1.56e-2	1.57e-2

results are in good agreement with those of Golmakani and Kadkhodayan (2011).

4.2 Convergence of GDQM

In order to study the convergence of the GDQM, the dimensionless deflection ($W_b = w_b/h$) for the annular and circular FG porous nanoplate is reported in Tables 4 and 5, respectively for different boundary conditions. Six types of boundary conditions for the annular nanoplate are considered namely as simply-simply (SS), clamped-clamped (CC), clamped-simply (CS), simply-clamped (SC), clamped-free (CF) and free-clamped (FC). As observed, by increasing the number of grid points, the convergent results are achieved. The number of terms, N = 17 is sufficient to give accurate results in Table 4.

Table 4 Convergence and accuracy of GDQM for deflection of annular nanoplate with Q = 2

N	CC	SC	CS	SS	FC	CF
7	0.1500	0.2550	0.548	0.807	0.924	1.387
11	0.3140	0.5338	1.277	1.860	2.435	3.652
13	0.4400	0.7481	2.002	2.886	4.211	6.317
15	0.4659	0.7921	2.183	3.139	4.691	7.036
17	0.4897	0.8325	2.364	3.389	5.183	7.774
19	0.4897	0.8325	2.364	3.389	5.183	7.774

Table 5 Convergence and accuracy of GDQM for deflection of circular nanoplate with l_0/h = 0.5

N	Clamped edge	Simply supported
7	109.32	153.048
11	20.642	28.898
13	12.921	18.089
15	2.0562	2.8787
17	0.3971	0.5559
19	0.3971	0.5559

4.3 Parametric study

Herein, the influences of different parameters on the dimensionless bending nonlinear displacement (W_b) versus dimensionless transverse load ($Q = q/E_m$) for the clamped annular nanoplate and material length scale parameter to thickness ratio for the circular nanoplate are shown. As expected, with increasing the dimensionless transverse load, the dimensionless nonlinear displacement is enhanced. In addition, with growing the material length scale parameter to thickness ratio, the dimensionless nonlinear displacement is decreased. It is due to the fact that with increasing the material length scale parameter to thickness ratio, the stiffness of the nanostructure is improved.

Figs. 3 and 4 present the effect of different boundary condition on the dimensionless nonlinear displacement for the annular and circular nanoplates, respectively. It is observed that in the annular nanoplate, the dimensionless nonlinear displacement is minimum for the annular nanoplate with CC and maximum for the CF boundary conditions. It is because the bending rigidity of the annular nanoplate with CC boundary condition is higher than other considered boundary conditions. In addition, the dimension-

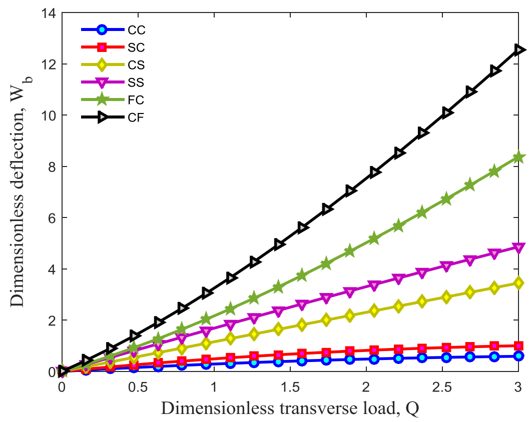

Fig. 3 The effect of different boundary conditions on the dimensionless nonlinear displacement for the FG porous annular nanoplate

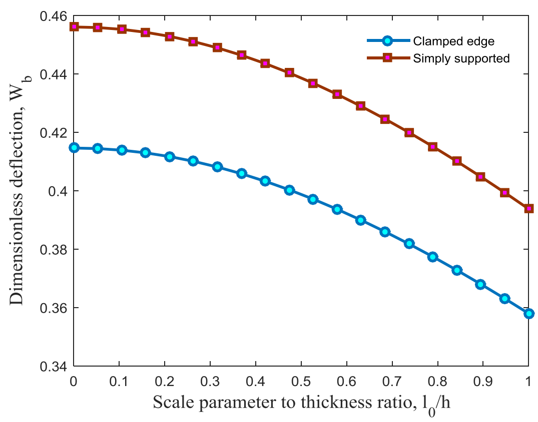

Fig. 4 The variation of the dimensionless nonlinear displacement of FG porous circular nanoplate with respect to l_0/h under two boundary condition

less nonlinear displacement for the SC and FC annular nanoplates is lower than CS and CF one. It shows that the effect of clamped boundary condition in the author surface of the annular nanoplate is higher than that in the inner surface. For instance, at $Q = 3$, the dimensionless nonlinear displacement for SC, FC, CS and CF annular nanoplates are 1.003, 8.366, 3.445 and 12.55, respectively. In the other words, the dimensionless nonlinear displacement for SC and FC annular nanoplates are 3.4 and 1.5 times lower those that of CS and CF annular nanoplates, respectively. The same as Fig. 3, in the Fig. 4, it can be concluded that the dimensionless nonlinear displacement for the clamped circular nanoplate is lower that simply supported ones.

The effect of material in-homogeneity parameter on the dimensionless nonlinear deflection is demonstrated in Figs. 5 and 6, respectively for annular and circular nanoplates, respectively. It can be found that with increasing the material in-homogeneity parameter, the material changes from ceramic ($p = 0$) and metal ($p = \infty$) and consequently the dimensionless nonlinear deflection increases. It is due to this fact that by enhancing the material in-homogeneity parameter, the stiffness of the annular/circular nanoplate reduces. For example, at $Q = 3$, the dimensionless nonlinear deflection of the ceramic annular nanoplate is 0.5027 while it is 0.9346 for the metal ones. As sketched, the dimensionless nonlinear deflection of the ceramic annular nanoplate is 85% lower than that of metallic ones. Furthermore, for the circular nanoplate at $l_0/h = 1$, changing the material in-homogeneity parameter from zero to infinite, the dimensionless nonlinear deflection is increased about 38%.

Figs. 7 and 8 indicate the effect of porosity on the dimensionless nonlinear deflection of the annular and circular nanoplates, respectively. It is shown that with increasing the porosity, the dimensionless nonlinear deflection is increased due to reduction in the stiffness of the structure. Furthermore, with increasing the applied load, the effect of porosity becomes more considerable. In another words, at $Q = 0.5$, the dimensionless nonlinear deflection of the porous annular nanoplate ($\xi = 0.8$) is 33% higher than perfect ($\xi = 0$) ones while for $Q = 3$, this percentage is about 50%. As sketched in Fig. 8, in circular nanoplate, the porosity effect is approximately independent to scale parameter to thickness ratio. For instance, at $l_0/h = 1$, the dimensionless nonlinear deflection of the porous annular nanoplate ($\xi = 0.8$) is 50% higher than the deflection of perfect ($\xi = 0$) annular nanoplate.

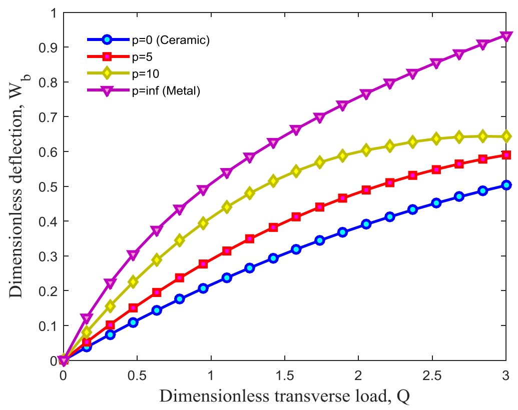

Fig. 5 The effect of material in-homogeneity parameter on the dimensionless nonlinear displacement for the FG porous annular nanoplate

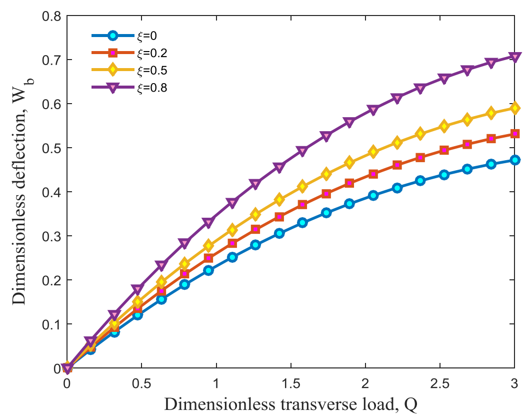

Fig. 7 The effect of porosity on the dimensionless nonlinear displacement for the FG porous annular nanoplate

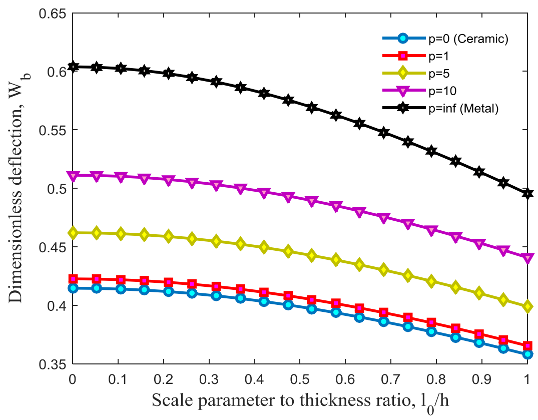

Fig. 6 The effect of material in-homogeneity parameter on the dimensionless nonlinear displacement for the FG porous circular nanoplate

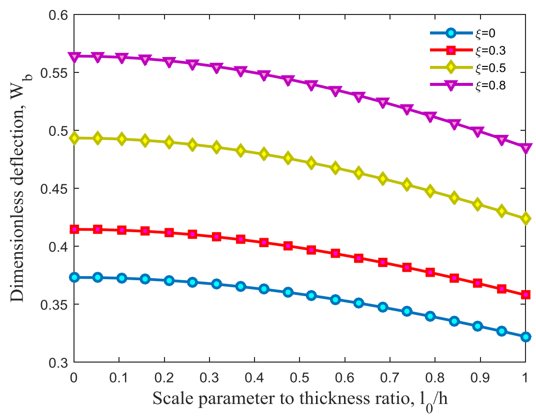

Fig. 8 The effect of porosity parameter on the dimensionless nonlinear displacement for the FG porous circular nanoplate

The effect of different elastic medium on the dimensionless nonlinear displacement for the annular and circular nanoplate is presented in Figs. 9 and 10, respectively. Four cases of without elastic medium, Winkler medium ($k_u \neq 0,\ k_l = k_s = 0$), Pasternak medium ($k_u \neq k_s \neq 0,\ k_l = 0$) and Kerr medium ($k_u \neq k_s \neq k_l \neq 0$) are considered. It can be seen that the dimensionless nonlinear displacement of the annular/circular without medium increases due to reduction in the stiffness of the structure. In addition, the dimensionless nonlinear displacement of the nanostructure with Kerr foundation is lower than Pasternak type and that is lower than Winkler ones. It is since in the Kerr medium, two spring and one shear constants are assumed while in the Pasternak medium we have one shear and spring constants and in the Winkler medium, there is only one spring element. Hence, the stiffness of the Kerr foundation is higher than Pasternak and Winkler mediums. In order to quantitative analysis of the results, at $Q = 3$, the dimensionless nonlinear displacement for the annular nanoplate resting on Kerr foundation is 0.5899 while it is 1.63 for the annular nanoplate without elastic medium. It shows that the Kerr foundation reduces the dimensionless nonlinear displacement 2.7 times with respect to the annular nanoplate without elastic medium.

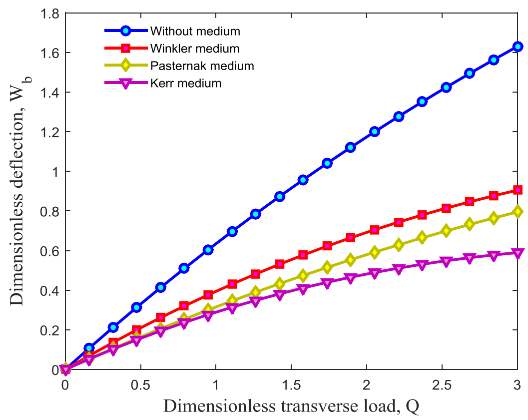

Fig. 9 The effect of elastic medium on the dimensionless nonlinear displacement for the FG porous annular nanoplate

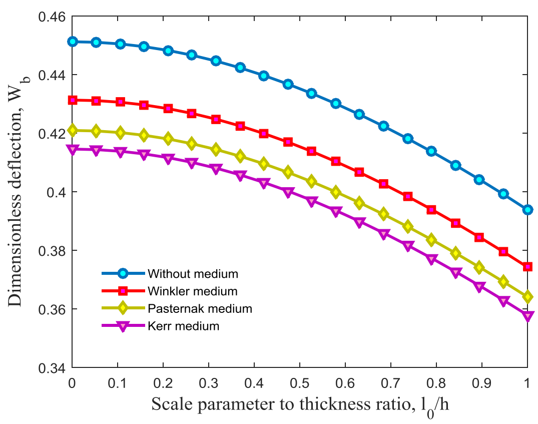

Fig. 10 The effect of elastic medium on the dimensionless nonlinear displacement for the FG porous circular nanoplate

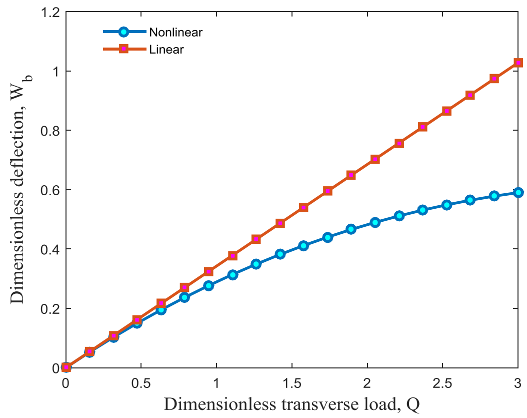

Fig. 11 The variation of linear and nonlinear deflection of FG porous annular nanoplate with respect to dimensionless transverse load (Q)

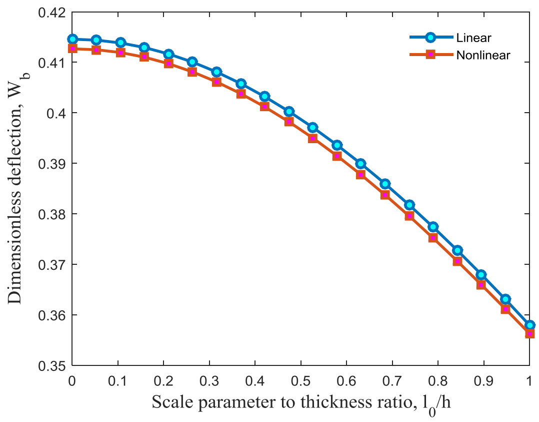

Fig. 12 The difference between the dimensionless nonlinear and linear deflection for the FG porous circular nanoplate

Figs. 11 and 12 illustrate the difference between the dimensionless nonlinear and linear deflection of the annular and circular nanoplates, respectively. By increasing Q, the deflection increases, leading to increasing the influence of nonlinear relations that causes the deflection in nonlinear situation to deviate from linear situation. It is indicated that the differences between the results of linear and nonlinear analysis grows by increasing Q. Another notable point concluded from Fig. 11 is that for $W_b < 0.4$, the difference between linear and nonlinear analysis is not significant when compared with $W_b > 0.4$.

5. Conclusions

This study was concerned with nonlinear bending analysis of FG porous annular/circular nanoplates resting on Kerr foundation. The size effects were proposed using MCST. Applying two refined plate theory, the governing equations were derived and using GDQM, the nonlinear deflection of the nanostructure was calculated for different boundary conditions. The effects of different parameters such as material length scale parameter, boundary condition, geometrical parameters of the nanoplate, elastic medium constants, porosity and FG index were shown on the nonlinear deflection of the annular/circular nanoplates. Numerical results show that the dimensionless nonlinear displacement for the SC and FC annular nanoplates was lower than CS and CF one. In the other words, the dimensionless nonlinear displacement for SC and FC annular nanoplates were 3.4 and 1.5 times lower than that of CS and CF annular nanoplates, respectively. With increasing the material in-homogeneity parameter, the dimensionless nonlinear deflection increases up to 85% at Q = 3 for the annular nanoplate and 38% for the circular ones at $l_0/h = 1$. It was shown that with increasing the porosity, the dimensionless nonlinear deflection was increased. With increasing the applied load, the effect of porosity becomes more considerable. In another words, at Q = 0.5, the dimensionless nonlinear deflection of the porous annular nanoplate ($\xi = 0.8$) was 33% higher than perfect ($\xi = 0$) ones while for Q = 3, this percentage was about 50%. The Kerr foundation reduces the dimensionless nonlinear displacement 2.7 times with respect to the annular nanoplate without elastic medium. In addition, the dimensionless nonlinear displacement of the nanostructure with Pasternak foundation was higher than Kerr type while the deflection of Kerr medium was lower than Winkler ones. Furthermore, the differences between the results of linear and nonlinear analysis rises up by increasing applied load. For W_b < 0.4, the difference between linear and nonlinear analysis is negligible whereas when W_b > 0.4, this discrepancy is significant.

References

Abbasi, S., Farhatnia, F. and Jazi, S.R. (2014), "A semi-analytical solution on static analysis of circular plate exposed to non-uniform axisymmetric transverse loading resting on Winkler elastic foundation", *Arch. Civil Mech. Eng.*, **14**, 476-488. https://doi.org/10.1016/j.acme.2013.09.007

Alibeigloo, A. (2018), "Thermo elasticity solution of functionally graded, solid, circular, and annular plates integrated with piezoelectric layers using the differential quadrature method", *Mech. Advan. Mater. Struct.*, **25**, 766-784. https://doi.org/10.1080/15376494.2017.1308585

Asemi, S.R., Farajpour, A., Asemi, H.R. and Mohammadi, M. (2014), "Influence of initial stress on the vibration of double-piezoelectric-nanoplate systems with various boundary conditions using DQM", *Physica E*, **63**, 169-179. https://doi.org/10.1016/j.physe.2014.05.009

Barati, M.R. (2017a), "Nonlocal-strain gradient forced vibration analysis of metal foam nanoplates with uniform and graded porosities", *Adv. Nano Struct., Int. J.*, **5**, 393-414. https://doi.org/10.12989/anr.2017.5.4.393

Barati, M.R. (2017b), "Nonlocal microstructure-dependent dynamic stability of refined porous FG nanoplates in hygro-thermal environments", *Eur. Phys. J. Plus*, **132**, 434-444. https://doi.org/10.1140/epjp/i2017-11686-2

Bahrami, A. and Teimourian, A. (2017), "Small scale effect on vibration and wave power reflection in circular annular nanoplates", *Compos. Part B: Eng.*, **109**, 214-226. https://doi.org/10.1016/j.compositesb.2016.09.107

Bedroud, M., Nazemnezhad, R., Hosseini-Hashemi, Sh. and Valixani, M. (2016), "Buckling of FG circular/annular Mindlin nanoplates with an internal ring support using nonlocal elasticity", *Appl. Math. Model.*, **40**, 3185-3210. https://doi.org/10.1016/j.apm.2015.09.003

Bellman, R. and Casti, J. (1971), "Differential quadrature and long-term integration", *J. Math. Anal. Appl.*, **34**, 235-238.

Chakraverty, S. and Behera, L. (2016), *Static and Dynamic Problems of nanobeams and nanoplates*, National Institute of Technology Rourkela, India.

Chan, D.Q., Anh, V.T.T. and Duc, N.D. (2019), "Vibration and nonlinear dynamic response of eccentrically stiffened functionally graded composite truncated conical shells in thermal environments", *Acta Mech.*, **230**, 157-178. https://doi.org/10.1007/s00707-018-2282-4

Dastjerdi, Sh., Jabbarzadeh, M. and Aliabadi, Sh. (2016), "Nonlinear static analysis of single layer annular/circular graphene sheets embedded in Winkler–Pasternak elastic matrix based on non-local theory of Eringen", *Ain Shams Eng. J.*, **7**, 873-884. https://doi.org/10.1007/s00707-018-2282-4

Duc, N.D. (2013), "Nonlinear dynamic response of imperfect eccentrically stiffened FGM double curved shallow shells on elastic foundation", *Compos. Struct.*, **99**, 88-96. https://doi.org/10.1016/j.compstruct.2012.11.017

Duc, N.D. (2016), "Nonlinear thermal dynamic analysis of eccentrically stiffened S-FGM circular cylindrical shells surrounded on elastic foundations using the Reddy's third-order shear deformation shell theory", *Eur. J. Mech. – A/Solids*, **58**, 10-30. https://doi.org/10.1016/j.euromechsol.2016.01.004

Duc, N.D., Khoa, N.D. and Thiem, H.T. (2018), "Nonlinear thermo-mechanical response of eccentrically stiffened Sigmoid FGM circular cylindrical shells subjected to compressive and uniform radial loads using the Reddy's third-order shear deformation shell theory", *Mech. Adv. Mater. Struct.*, **25**, 1157-1167. https://doi.org/10.1080/15376494.2017.1341581

Ebrahimi, F. and Heidari, E. (2017), "Surface effects on nonlinear vibration of embedded functionally graded nanoplates via higher order shear deformation plate theory", *Mech. Adv. Mat. Struct.*, **26**(8), 671-699. https://doi.org/10.1080/15376494.2017.1410908

Ebrahimi, F. and Heidari, E. (2018), "Vibration characteristics of advanced nanoplates in humid-thermal environment incorporating surface elasticity effects via differential quadrature method", *Struct. Eng. Mech., Int. J.*, **68**(1), 131-157. https://doi.org/10.12989/sem.2018.68.1.131

Farhatnia, F., Ghanbari-Mobarakeh, M., Rasouli-Jazi, S. and Oveissi, S. (2017), "Thermal buckling analysis of functionally graded circular plate resting on the pasternak elastic foundation via the differential transform method", *Facta Universitatis, Series: Mech. Eng.*, **15**, 545-563. https://doi.org/10.22190/FUME170104004F

Farhatnia, F., Babaei, J. and Foroudastan, R. (2018), "Thermo-Mechanical nonlinear bending analysis of functionally graded thick circular plates resting on Winkler foundation based on sinusoidal shear deformation theory", *Arab. J. Sci. Eng.*, **43**, 1137-1151. https://doi.org/10.1007/s13369-017-2753-2

Ghadiri, M., Shafiei, N. and Alavi, H. (2017), "Thermo-mechanical vibration of orthotropic cantilever and propped cantilever nanoplate using generalized differential quadrature method", *Mech. Adv. Mater. Struct.*, **24**, 636-646. https://doi.org/10.1080/15376494.2016.1196770

Golmakani, M.E. and Kadkhodayan, M. (2011), "Nonlinear bending analysis of annular FGM plates using higher-order shear deformation plate theories", *Compos. Struct.*, **93**, 973-982. https://doi.org/10.1016/j.compstruct.2010.06.024

Golmakani, M.E. and Vahabi, H. (2017), "Nonlocal buckling analysis of functionally graded annular nanoplates in an elastic medium with various boundary conditions", *Microsyst. Technol.*, **23**, 3613-3628. https://doi.org/10.1007/s00542-016-3210-y

Hajmohammad, M.H., Zarei, M.Sh., Sepehr, M. and Abtahi, N. (2018), "Bending and buckling analysis of functionally graded annular microplate integrated with piezoelectric layers based on layerwise theory using DQM", *Aerosp. Sci. Technol.*, **79**, 679-688. https://doi.org/10.1016/j.ast.2018.05.055

Jung, W.Y., Han, S.Ch. and Park, W.T. (2014), "A modified couple stress theory for buckling analysis of S-FGM nanoplates embedded in Pasternak elastic medium", *Compos.: Part B*, **60**, 746-756. https://doi.org/10.1016/j.compositesb.2013.12.058

Karami, B. and Janghorban, M. (2016), "Effect of magnetic field on the wave propagation in nanoplates based on strain gradient theory with one parameter and two-variable refined plate theory", *Modern Phys. Lett. B*, **30**, 1650421, 17 pages. https://doi.org/10.1142/S0217984916504212

Karami, B., Janghorban, M., Shahsavari, D. and Tounsi, A. (2018), "A size-dependent quasi-3D model for wave dispersion analysis of FG nanoplates", *Steel Compos. Struct., Int. J.*, **28**(1), 99-110. https://doi.org/10.12989/scs.2018.28.1.099

Karimi, M. and Shahidi, A.R. (2017), "Thermo-mechanical vibration, buckling, and bending of orthotropic graphene sheets based on nonlocal two-variable refined plate theory using finite difference method considering surface energy effects", *Proc. IMechE Part N: J. Nanomater., Nanoeng. Nanosyst.*, **231**, 111-130. https://doi.org/10.1177/2397791417719970

Karlicic, D., Murmu, T., Adhikari, S. and McCarthy, M. (2015), *Non-local Structural Mechanics*, John Wiley & Sons, USA.

Limkatanyu, S., Prachasaree, W., Damrongwiriyanupap, N., Kwon, M. and Jung, W. (2013), "Exact stiffness for beams on Kerr-Type foundation: the virtual force approach", *J. Appl. Mathemat.*, **13**, 626287, 13 pages. http://dx.doi.org/10.1155/2013/626287

Narendar, S. (2011), "Buckling analysis of micro-/nano-scale plates based on two-variable refined plate theory incorporating nonlocal scale effects", *Compos. Struct.*, **93**, 3093-3103. https://doi.org/10.1016/j.compstruct.2011.06.028

Narendar, S. and Gopalakrishnan, S. (2012), "Scale effects on buckling analysis of orthotropic nanoplates based on nonlocal two-variable refined plate theory", *Acta Mech.*, **223**, 395-413. https://doi.org/10.1007/s00707-011-0560-5

Ma, L.S. and Wang, T.J. (2004), "Relationship between axisymmetric bending and buckling solutions of FGM circular plates based on third-order plate theory and classical plate theory", *Int. J. Solids Struct.*, **41**, 85-101. https://doi.org/10.1016/j.ijsolstr.2003.09.008

Malekzadeh, P. and Shojaee, M. (2013a), "A two-variable first-order shear deformation theory coupled with surface and nonlocal effects for free vibration of nanoplates", *J. Vib. Cont.*, **21**, 2755-2772. https://doi.org/10.1177/1077546313516667

Malekzadeh, P. and Shojaee, M. (2013b), "Free vibration of nanoplates based on a nonlocal two-variable refined plate theory", *Compos. Struct.*, **95**, 443-452. https://doi.org/10.1016/j.compstruct.2012.07.006

Mecha, I., Mechab, B., Benaissa, S., Serier, B. and Bachir Bouiadjra, B. (2016), "Free vibration analysis of FGM nanoplate with porosities resting on Winkler Pasternak elastic foundations based on two‑variable refined plate theories", *J. Brazil. Soc. Mech. Sci. Eng.*, **38**, 2193-2211. https://doi.org/10.1007/s40430-015-0482-6

Paliwal, D.N. and Ghosh, S.K. (2014), "Stability of orthotropic plates on a Kerr foundation", *AIAA J.*, **38**, 1994-1997. https://doi.org/10.2514/2.859

Phadikar, J.K. and Pradhan, S.C. (2010), "Variational formulation and finite element analysis for nonlocal elastic nanobeams and nanoplates", *Computat. Mat. Sci.*, **49**, 492-499. https://doi.org/10.1016/j.commatsci.2010.05.040

Poodeh, F., Farhatnia, F. and Raeesi, M. (2018), "Buckling analysis of orthotropic thin rectangular plates subjected to nonlinear in-plane distributed loads using generalized differential quadrature method", *Int. J. Computat. Meth. Eng. Sci. Mech.*, **19**, 102-116. https://doi.org/10.1080/15502287.2018.1430077

Quan, T.Q., Tran, P., Tuan, N.D. and Duc, N.D. (2015), "Nonlinear dynamic analysis and vibration of shear deformable eccentrically stiffened S-FGM cylindrical panels with metal-ceramic-metal layers resting on elastic foundations", *Compos. Struct.*, **126**, 16-33. https://doi.org/10.1016/j.compstruct.2015.02.056

Rajasekaran, S. (2017), "Analysis of non-homogeneous orthotropic plates using EDQM", *Struct. Eng. Mech., Int. J.*, **61**(2), 295-316. https://doi.org/10.12989/sem.2017.61.2.295

Rahimi Pour, H., Vossough, H., Heydari, M.M., Beygipoor, Gh. and Azimzadeh, A. (2015), "Nonlinear vibration analysis of a nonlocal sinusoidal shear deformation carbon nanotube using Differential quadrature method", *Struct. Eng. Mech., Int. J.*, **54**(6), 1063-1071. https://doi.org/10.12989/sem.2015.54.6.1061

Reddy, J.N., Wang, C.M. and Kitipornchai, S. (1999), "Axisymmetric bending of functionally graded circular and annular plates", *Eur. J. Mech. A – Solids*, **18**, 185-199. https://doi.org/10.1016/S0997-7538(99)80011-4

Rezaei, A.S. and Saidi, A.R. (2018), "An analytical study on the free vibration of moderately thick fluid-infiltrated porous annular sector plates", *J. Vib. Cont.*, **24**, 4130-4144. https://doi.org/10.1177/1077546317721416

Robinson, M.T.A. (2018), "Analysis of the vibration of axially moving viscoelastic plate with free edges using differential quadrature method", *J. Vib. Control*, **24**(17), 3908-3919. https://doi.org/10.1177/1077546317716316

Saidi, A.R., Rasouli, A. and Sahraee, S. (2009), "Axisymmetric bending and buckling analysis of thick functionally graded circular plates using unconstrained third-order shear deformation plate theory", *Compos. Struct.*, **89**, 110-119. https://doi.org/10.1016/j.compstruct.2008.07.003

Shahsavari, D., Karami, B. and Li, L. (2018), "A high-order gradient model for wave propagation analysis of porous FG nanoplates", *Steel Compos. Struct., Int. J.*, **29**(1), 53-66. https://doi.org/10.12989/scs.2018.29.1.053

Shimpi, R.P. and Patel, H.G. (2006), "A two variable refined plate theory for orthotropic plate analysis", *Int. J. Solids Struct.*, **43**, 6783-6799. https://doi.org/10.1016/j.ijsolstr.2006.02.007

Shokrani, M.H., Karimi, M., Salmani Tehrani, M. and Mirdamadi, H.R. (2016), "Buckling analysis of double-orthotropic nanoplates embedded in elastic media based on non-local two-variable refined plate theory using the GDQ method", *J. Brazil. Soc. Mech. Sci. Eng.*, **38**, 2589-2606. https://doi.org/10.1007/s40430-015-0370-0

Sobhy, M. (2016), "Hygrothermal vibration of orthotropic double-layered graphene sheets embedded in an elastic medium using the two-variable plate theory", *Appl. Math. Model.*, **40**, 85-99. https://doi.org/10.1016/j.apm.2015.04.037

Sobhy, M. (2017), "Hygro-thermo-mechanical vibration and buckling of exponentially graded nanoplates resting on elastic foundations via nonlocal elasticity theory", *Struct. Eng. Mech., Int. J.*, **63**(3), 401-415. https://doi.org/10.12989/sem.2017.63.3.401

Teifouet, M. and Robinson, A. (2017), "Analysis of the vibration of axially moving viscoelastic plate with free edges using differential quadrature method", *J. Vib. Cont.*, **24**, 3908-3919. https://doi.org/10.1177/1077546317716316

Xu, W., Wang, L. and Jiang, J. (2016), "Strain gradient finite element analysis on the vibration of double-layered graphene sheets", *Int. J. Computat. Meth.*, **13**, 1650011, 18 pages. https://doi.org/10.1142/S0219876216500110

CC